Nanoscale

PAPER

View Article Online
View Journal

Cite this: DOI: 10.1039/d4nr03966a

Graphene or MoS_2 nanopores: pore adhesion and protein linearization†

Peijia Wei, * Mayukh Kansari and Maria Fyta

Nanopores drilled in materials can electrophoretically drive charged biomolecules to enable their detection. Here, we explore and compare two-dimensional nanopores, graphene and MoS_2, in order to unravel their advantages and disadvantages with regard to protein detection. We tuned the protein translocation and its dynamics by the choice and concentration of the surrounding solvent. For this, we used a typical monovalent salt solution, as well as a molecular solution. We assessed, with the aid of atomistic simulations, the efficiency of both nanopores in threading the protein on the basis of measurable ionic current signals. In the case of graphene, the protein adheres on the graphene surface, hindering the translocation under physiological conditions. This stickiness is resolved with the addition of a denaturant by the formation of a hydrophilic cationic layer on the pore surface and the protein can thread the pore in a linearized configuration. On the other hand, the MoS_2 nanopores can thread the protein also in a physiological solution, leading to longer passage times, while the degree of protein linearization is lower than in the case of graphene in a molecular solution. We analyze the differences between the two nanopore materials on the basis of the complex molecular interactions between all components, the material, the target protein, and the solvent. We discuss the relevance of the results with respect to controlling the protein dynamics and enhancing the read-out ionic signals in view of an efficient detection of proteins through 2D nanopores.

Received 27th September 2024,
Accepted 12th December 2024

DOI: 10.1039/d4nr03966a

rsc.li/nanoscale

1 Introduction

Nanopores are nanometer-sized openings in materials that can be placed in a solution and thread biomolecules, giving rise to an efficient single-molecule technique. In this case, the analyte of interest (*e.g.*, DNA, RNA, and protein) is driven by an applied electric field and transported through the nanopore in an electrolyte solution. A sensor measures changes in the generated ionic current as the molecule moves through the nanopore and can potentially read-out the sequence of the analyte.[1] Specifically, 2D materials, such as graphene[2] and molybdenum disulfide (MoS_2),[3] apart from all their other applications can also be fabricated as nanopores and used to thread biomolecules.[4–6] The thickness of single-layer graphene is only 0.34 nm,[7] which is comparable to the distance between two nucleobases in DNA or the inter amino acid spacing in proteins. This match indicates a high potential for graphene nanopores to be utilized in achieving high-resolution protein detection and sequencing. Besides graphene, single-layer molybdenum disulfide (MoS_2) nanopores have also emerged as a promising technology for nanopore sequencing for proteins and nucleic acids due to their unique properties and atomic-scale thickness, providing a means to measure both ionic and electronic currents at the same time.[8–10] MoS_2 nanopores offer high sensitivity and resolution for detecting individual amino acids in polypeptide chains and nucleosides in DNA/RNA. Recent studies[11,12] have demonstrated the potential of MoS_2 nanopores for protein sequencing applications. The direct experimental identification of single amino acids using atomically engineered MoS_2 nanopores, achieving sub-1 Dalton resolution for discriminating chemical group differences and even recognizing amino acid isomers, has been reported.[11] This ultra-confined nanopore system was also used to detect phosphorylation of individual amino acids, showcasing its capability for determining post-translational modifications. At the same time, extensive molecular dynamics simulations and machine learning techniques have demonstrated that nanoporous single-layer MoS_2 can detect individual amino acids in a polypeptide chain with high accuracy and distinguishability.[12] These findings suggest that MoS_2 nanopores have significant potential for advancing protein sequencing technology and enabling single-molecule level chemical recognition.

Many simulation studies (both quantum and classical levels) have found that both DNA[13,14] and proteins[15–17] can be

Computational Biotechnology, RWTH Aachen University, Worringerweg 3, 52074 Aachen, Germany. E-mail: pwei@biotec.rwth-aachen.de

† Electronic supplementary information (ESI) available. See DOI: https://doi.org/10.1039/d4nr03966a

driven through graphene nanopores by an electric field and exhibit step-wise translocation, which is beneficial for single-resolution identification. This step-wise behavior of the translocation process is attributed to the "stickiness" of hydrophobic graphene that promotes the adhesion of the DNA/protein units on its surface due to the π–π interactions formed.[18] However, only a few experimental studies have reported achieving protein sequencing using graphene nanopores. The stickiness of graphene could be one of the factors that hinders the protein translocation. Efforts have been made to solve this stickiness by chemically modifying the surface, for example, with polyethylene glycol (PEG),[19,20] pulling the protein using an AFM probe tip,[21] or by designing complex nanopore setups (*e.g.*, stacking graphene with MoS_2).[22] Along these lines, whether simply optimizing the electrolyte could solve the stickiness and thus enhance the translocation of proteins through graphene nanopores has, to our knowledge, not been pointed out before.

The need for nanopore-based protein sequencing arises from the demand for high-resolution, real-time analysis of protein sequences and mainly the detection of post-translational modifications in these protein sequences, pointing to diseases.[23] For this detection, however, significant challenges still remain. These include the accurate interpretation of complex signals generated by diverse amino acids[24] and the management of protein denaturation and unfolding during the sequencing process.[25] For the latter, it was found that adding the protein denaturant guanidinium chloride (GdmCl)[26] to the solution in the case of a biological α-hemolysin nanopore could assist protein unfolding during translocation.[27] This unfolding should overcome the strong intramolecular interactions within proteins to enable a single-file translocation, during which amino acids on the protein chain pass through the nanopore one at a time in a linear, sequential arrangement. Challenges still exist in this context as proteins, in contrast to DNA and RNA, are not uniformly charged and the application of the electric field across a nanopore cannot ensure a unidirectional protein transport, which significantly influences the detection accuracy.[28,29]

Motivated by the above points, we model two-dimensional nanopores, graphene and MoS_2, translocating a protein and investigate in detail the influence of the type and concentration of the surrounding solvent on the translocation dynamics and the resulting ionic current signals. We assess the pathways to tune the translocation speed and guide the detection process by investigating the nanopore material and the solvent details, as well as how these interact with the translocating protein to steer it through the pore and provide detectable signatures in the ionic current signals. Our specific focus is a comparison of the nanopore material, graphene or MoS_2, with respect to the translocation dynamics and the detection characteristics. To this end, we begin with an outline of the computational methodology used in Section 2, continue with the discussion of the results in Section 3 and conclude with a summary of our findings and their impact.

2 Methodology

The 2D nanopores are modelled here with Molecular Dynamics (MD) using the Gromacs 2022.3 simulation package[30] with periodic boundary conditions and an integration time step of 2 fs. The CHARMM36 force-field[31] is used for all components, material pores, proteins, and solvent species. The TIP3P[32] model modified for the CHARMM force field is used for water. The force fields have been tested and are typically used in biomolecular simulations to accurately capture the dynamic behavior and interactions of these molecules in complex environments.[33–35] The temperature of the simulation system was maintained at 300 K using a velocity rescaling thermostat[36] with a coupling constant of 1 ps. For the simulations including the MoS_2 nanopore, the thermostat could not sustain the input temperature of 300 K. To this end, for the MoS_2 simulations, we used the Nose–Hoover thermostat with a different coupling constant for different elements in order to keep the temperature at 300 K (details can be found in the ESI†). For all systems, we performed energy minimization followed by two equilibration steps including 2 ns of (NVT) simulations and 30 ns of (NPT) simulations. For the NPT equilibration, the pressure was kept at 1 bar using a semi-isotropic Parrinello–Rahman barostat[37] applied along the *z*-direction (see Fig. 1 for the axes description). The LINCS algorithm[38] was adopted to enforce constraints on the bonds involving hydrogen atoms, while the particle mesh Ewald (PME) algorithm[39] was used to calculate the electrostatic interactions with a cutoff distance of 1.2 nm. During the equilibration steps, the α carbon (C_α) atom of the amino acid

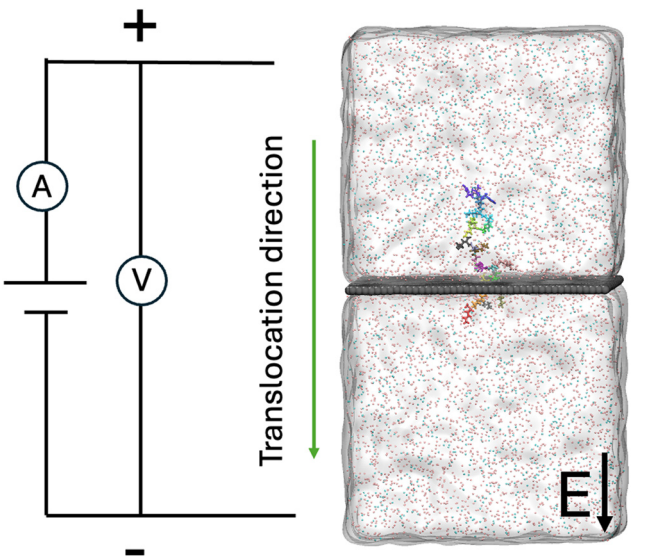

Fig. 1 A typical setup of the computational box used in the simulations. The *cis* and *trans* sides of the chambers are given, as well as the direction of the applied electric field $\vec{E}$. The translocating histone H4 protein segment is also shown, while the solvent composed of 1 M KCl is mapped through a semitransparent surface. The potassium and chloride ions are shown as pink and cyan spheres, respectively.

located at the middle of the nanopore was harmonically restrained with a force constant of 10^4 (cal mol^{-1} Å^{-2}). This restraint ensured that the target H4 protein segment did not drift out of the pore prior to the application of the electric field and that the translocation of this and not the trailer lysine molecule was monitored from time 0 fs on. Each atom of the nanopore sheet was restrained to its initial coordinates using a harmonic spring with a force constant of 10^4 (cal mol^{-1} Å^{-2}). Production runs of 500 ns (530 ns for the MoS_2 nanopore with GdmCl) were performed under an applied electric field along the z-direction, with a field strength of $E = -V/L_z$, where V is the target transmembrane bias and L_z is the length of the simulation box in the z-direction. The restraint applied to the protein was removed during this part to allow the translocation.

Two different 2D materials, graphene and MoS_2, are considered for generating the nanopore. The efficiency of these materials, and the advantages and disadvantages in the translocation process, will be compared in this work. The graphene nanopore with a diameter of 1.5 nm was opened on a graphene sheet with the dimensions 10 nm × 10 nm generated using VMD's[40] nanotube builder plugin. The MoS_2 nanopore was opened in a 1T MoS_2 sheet that we had optimized in advance before opening the pore. Due to the different bonding lengths and characteristics in MoS_2, for this material, the diameter was set to 1.6 nm. All atoms within a circle $x^2 + y^2 < R^2$ were removed as also performed elsewhere,[15] where R was set to 0.75 nm for graphene and 0.8 nm for MoS_2. The graphene nanopore has a hexagonal shape aligning with the hexagonal lattice structure. The MoS_2 pore has a nearly hexagonal shape due to the different symmetries and structures of the MoS_2 material. Since this is a heteroatomic material, the pore could not be completely symmetric and hexagonal and had a slightly distorted hexagonal shape. The pore shapes were, though, made as similar as possible. The size of the computational box was initially set at 11.5 × 11.5 × 18.0 nm^3 for both nanopore materials. Note that though the two materials have different atomic arrangements and lattice constants, we have constructed the nanopores avoiding stressing the materials and ensuring that the overall surface sizes, but not the number of atoms, were very similar. Regarding the charges on the nanopore material, graphene has a neutral surface (the carbon atoms are not charged), while the MoS_2 layer is negatively charged with the Mo and S atoms carrying a charge of +0.5e and −0.25e, respectively, resulting in a net negative charge of the MoS_2 nanopore material of −38.5e.

In order to probe the characteristics of the two nanopore materials in threading biomolecules, we have used the first 20 residues of the histone H4 protein with the sequence N′-MSGRGKGGKGLGKGGAKRHR-C′ as a target analyte. Five lysine (K) amino acids, which are positively charged, were added to the N′-terminus of the target protein as a trailer molecule. Due to its large charge, this trailer molecule is expected to strongly interact with the electric field in order to efficiently translocate the pore and drag the target H4 protein with it. The latter, made of many neutral amino acids (M, S, G, and L), does not strongly interact with the electric field and thus does not easily pass through the pore. Initially, the protein was placed inside the nanopore, with the trailer K (lysine) molecule already threaded through, aiming solely at the translocation of the target and at the same time save computational time. For a systematic assessment of the influence of different factors on the translocation of the H4 peptide through the nanopores, we modelled different solvent types and concentrations. We began with the translocation under normal physiological conditions of a KCl solution. For this, we modelled KCl concentrations of 0.5 M, 1 M, and 3 M for the graphene nanopore and 1 M for the MoS_2 nanopore. We continued with a protein denaturant, choosing the molecular solute GdmCl at concentrations of 3 M and 5 M in the case of the graphene nanopore and 3 M with the MoS_2 nanopore. GdmCl was added to the 1 M KCl solution. The influence of the GdmCl solutes on the protein was assessed by checking the conformation of the protein chain in solution with 1 M, 2 M, and 3 M GdmCl added to 1 M KCl solution for the graphene nanopore. The general setup used in our simulations is depicted in Fig. 1. An electric field of 1 V was applied in all MD simulations. This value is higher than the experimental one. However, such a larger voltage is typically used in simulations to facilitate tracking the translocation process and dynamics within the accessible time scales of the simulations.

The ionic current through the nanopore is the observable that is measured experimentally and can be used to monitor the translocation of any target molecule through the nanopore.[41,42] Accordingly, in our analysis, we calculated the ionic current, $I(t)$, through the nanopore using the following equation:

$$I(t) = \frac{1}{\Delta t L_Z} \sum_{i=1}^{N} q_i [z_i(t + \Delta t_I) - z_i(t)], \quad (1)$$

where Δt_I is a time window set at 2 ps, L_Z is the length of the simulation box along the z-direction, N is the total number of ions passing through the nanopore during simulation, and z_i and q_i are the ion's z-coordinate and charge, respectively.[43] For evaluation of the protein conformation, we calculated the radius of gyration as follows:

$$R_g(x) = \sqrt{\frac{1}{M_p} \sum_{i=1}^{N_p} m_i (r_{i,p} - R_{p,COM})^2}, \quad (2)$$

where $M_p = \sum_{i=1}^{N_p} m_i$ is the total mass of all N_p atoms in the protein, $r_{i,p}$ is the position of each atom in the protein, and $R_{p,COM} = \frac{1}{N_p} \sum_{i=1}^{N_p} r_i$ is the center of mass of the protein chain. The influence of the solvent on the translocation process was monitored through the radial distribution functions (RDFs), which are a measure of the probability of finding a particle at a given distance from a reference particle. The RDFs can thus map the specific intramolecular interactions within the nano-

pore–protein–solution system. Finally, the mean squared displacement (MSD) was computed from the MD trajectories and is a measure of the mobility and diffusion of all species, water, ions, and proteins.

3 Results

We begin the analysis by elucidating the main differences of the graphene and MoS_2 nanopores in threading through the histone H4 protein. This will be based on interaction and structural details in both cases and include the contributions of all the different components in the system, the material pore, protein, water, and ions. The most important aspects addressed below are the translocation dynamics of the target analyte, that is the speed of the protein threading the pore and its conformation therein. For the latter, the protein is expected to be linearized in order for its sequence or/and identity to be detected using the nanopore concept.

3.1 Resolving graphene stickiness

One of the major indications of the need for tuning the detection with graphene nanopores is the reported[44–46] adhesion of the analytes on the graphene surface. This adhesion of, mainly, the aromatic units of DNA, RNA, and proteins on the graphene surface either halts or hinders the translocation, thereby affecting detection.[18] In our simulations, we monitored the protein sticking on the graphene nanopore surface during translocation in pure KCl solutions of 0.5 M, 1 M, and 3 M causing a slow, non-uniform and occasionally bidirectional translocation. Hairpin protein conformations are observed in the 3 M KCl solution hindering the translocation for more than 180 ns. We quantified and compared the observed adhesion for our target histone H4 protein on the surface by calculating the number of amino acids that adhere to the top surface of the two nanopores, graphene and MoS_2, modelled here. At the same time, we also compared the adhesion for different solvent types and concentrations. An amino acid is considered to be adhered to the nanopore surface if its center of mass is located within 0.5 nm distance from the surface.[15] A comparison of the amino acid adhesion on the two materials and the different conditions during the translocation process is summarized in Fig. 2(a). Note that an amino acid is considered as adhered to the nanopore surface if its center of mass is located within 5 Å of the nearest membrane atom and is positioned outside the nanopore. As a first observation, the adhesion of the protein on the two nanopore materials is on average very similar in a 1 M KCl solution. Once the molecular ion Gdm^+ is added to the KCl solution, a decrease of around 40% in the number of adhered amino acids can be observed for the graphene pore and becomes larger in the MoS_2 pore. The decrease is even more pronounced when the GdmCl concentration is increased, as evident for the translocation through the graphene nanopore. The higher curve for the 3 M GdmCl + 1 M KCl solution and graphene compared to that of MoS_2 is assigned to the differences in the translocation characteristics. As the protein segment is translocating through the graphene nanopore, more amino acids on the protein segment come closer to the membrane and increase the possibility of adhering on it, and thus the number of adhered amino acids. The overall adhesion, though, remains much lower compared to that in the pure KCl solution throughout the translocation, highlighting the effectiveness of GdmCl in reducing interactions between the protein segment and the graphene surface. In the 5 M GdmCl + 1 M KCl solution and graphene, the high GdmCl concentration more effectively covers the graphene nanopore, preventing almost any amino acid from adhering to it throughout the translocation process. Beyond that and from ~250 ns on, the number of adhered amino acids reaches a value of 2 as the glycine residues G13 and G15 keep fluctuating very close to

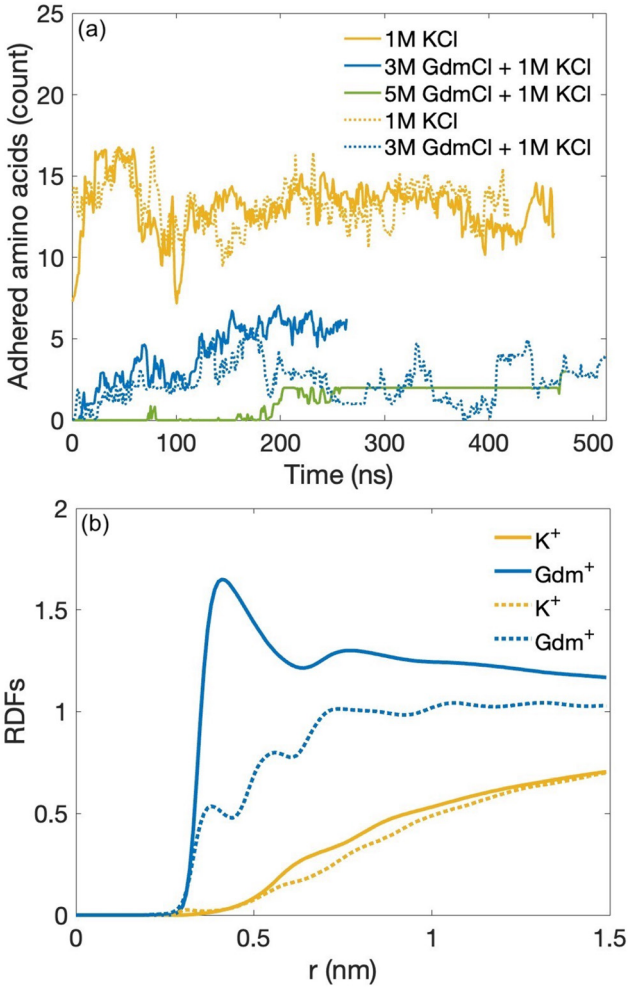

Fig. 2 (a) The number of amino acids adhered to the graphene (solid lines) or MoS_2 (dotted lines) surface in different solutions during the translocation process averaged by every 1 ns. (b) Radial distribution functions (RDFs) between the cations and the material pore. The cases for the Gdm^+ ions (in a 1 M KCl solution added with 3 M GdmCl) and K^+ ions (in a 1 M KCl solution) are depicted in blue and yellow, respectively. The results for the graphene and the MoS_2 nanopores are shown by the solid and dotted lines, respectively.

the graphene surface. The respective differences throughout the translocation process are visualized in Fig. S2 of the ESI.†

This softening of the protein–material interactions is apparently directly connected with the presence of the molecular guanidinium cation that somehow prevents the protein from sticking to the material. With the aim of understanding the details behind these interactions, we calculated the radial distribution functions (RDFs) between the solutes and the material for both graphene and MoS_2 and they are shown in Fig. 2(b). We specifically provide through the RDFs the interactions between the cations (K^+ or Gdm^+) in the 1 M KCl or 3 M GdmCl + 1 M KCl solution and the material surface. A significant peak at around 0.4 nm can be seen in the RDF between the graphene and the guanidinium cations, emphasizing that the Gdm^+ strongly accumulates at around 0.4 nm from the graphene surface due to its π–π interaction with the carbon rings of the surface, thus forming a cation-rich layer on the surface. In this way, the hydrophobic graphene surface is covered by a thin Gdm^+-rich hydrophilic layer that hinders the formation of the strong π–π interaction with the analyte. In contrast, for MoS_2, this is not observed, as also indicated by the respective RDF curves, which map the electrostatic interactions of MoS_2 with the Gdm^+. These are less strong and more long range than those of the graphene–Gdm^+ RDFs. For comparison, the RDFs between the two material pores and the potassium cations are given in the figure in order to underline the respective long-range interactions that would not intermingle in the stronger and short-range π–π protein–material interactions.

3.2 Linearizing the protein

Having resolved the adhesion challenges, especially when utilizing graphene nanopores, we moved to the next challenge, namely the conformation for the translocating protein. For detecting the sequence or patterns within any biomolecule, it is necessary to expose its units (nucleobases or amino acids) to the inner pore surface in order for them to be detected. As we also observed in our simulations with the KCl solution, the translocating protein is rather coiled or compact and passes through the pore in that manner. For resolving this, the protein needs to be linearized either before entering or while translocating the pore. In order to quantify the degree of linearization of the protein during the translocation process and in the electrolyte chambers, we used the radius of gyration (R_g) as a measure of the form of protein conformation.[47,48] The radius of gyration of the histone H4 protein in the nanopores, averaged over 30 ns of the NPT equilibrium step, is depicted in Fig. 3 for the different electrolyte solutions and nanopores. (The respective time evolution can be found in the ESI.†) The respective average R_g values of the protein backbone at 0 M, 3 M and 5 M GdmCl concentrations were found to be 1.34, 1.53, and 1.57 nm in the case of the graphene nanopore and 1.14 and 1.21 nm at 0 M and 3 M GdmCl concentrations in the MoS_2 case. There is a clear trend of obtaining more open protein conformations as more GdmCl is added to the solution, which was confirmed for both nanopores. Overall, the

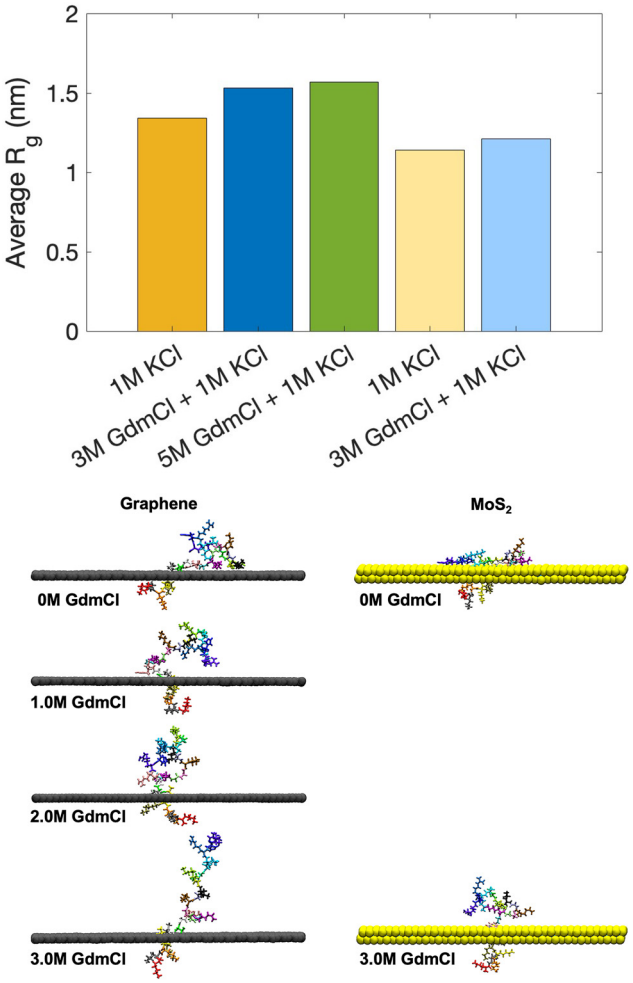

Fig. 3 (Top) The average radius of gyration (R_g) of the backbone atoms in the protein during 30 ns of NPT equilibrium in the graphene (dark colors) and the MoS_2 (light colors) nanopores. The solution is marked in the *x*-axis. (Bottom) Snapshots illustrating the protein conformations in different solution environments.

average radius of gyration of the protein is lower in the case of the MoS_2 pores for all solution types. This originates from the fact that the MoS_2 surface is negatively charged, promoting electrostatic interactions with the protein through the charged amino acids of the latter. This is not the case with graphene in 1 M KCl, for which the larger stretch (larger R_g) comes from the strong dispersion interactions and the corresponding sticking of the protein on the material. As a result, part of the protein is pulled by the electric field through the pore, while it is partly sticking on the *cis*-part of the graphene. Accordingly, the protein is being stretched by these opposing forces. In the electrolyte solutions including GdmCl, the dispersion interactions are less strong due to the formation of the Gdm^+ hydrophilic layer discussed above. In these cases, the linearization is imposed by the denaturant solute. The radius of gyration results suggests that the protein undergoes less tight packing with a higher concentration of GdmCl added to the 1 M KCl solution for both nanopores. In other words, GdmCl

promotes stretching, *i.e.* linearization, of the protein which is of high importance in order to enhance the signal-to-noise ratio in the ionic currents used for read-out.

To offer more insight into the mechanisms that are related to a linearized (or not) protein conformation, we directly analyzed its interactions with the ions in the solutions by calculating the average number of hydrogen bonds formed and the radial distribution functions. GdmCl was discovered to effectively compete with water in the formation of hydrogen bonds as inferred from the bar plot in Fig. 4(a). The average numbers of hydrogen bonds between the protein and water molecules were found to be 84, 64 and 54 in 1 M KCl solution with 0 M, 3 M and 5 M GdmCl in the graphene nanopore and 84 and 65 in 1 M KCl solution with 0 M and 3 M GdmCl in the MoS_2 nanopore, while the average number of hydrogen bonds between the protein and GdmCl molecules turned out to be 12 and 15 in 1 M KCl solution with 3 M and 5 M GdmCl in the graphene nanopore and 11 in 1 M KCl solution with 3 M GdmCl in the MoS_2 nanopore. (The respective bar plot and the time evolution can be found in the ESI.†) Apparently, the addition of GdmCl to the KCl electrolyte solution hinders the formation of hydrogen bonds between the protein and water. At the same time, the increase in the concentration of GdmCl in the solution promotes the formation of hydrogen bonds between the molecular solvent and the protein.

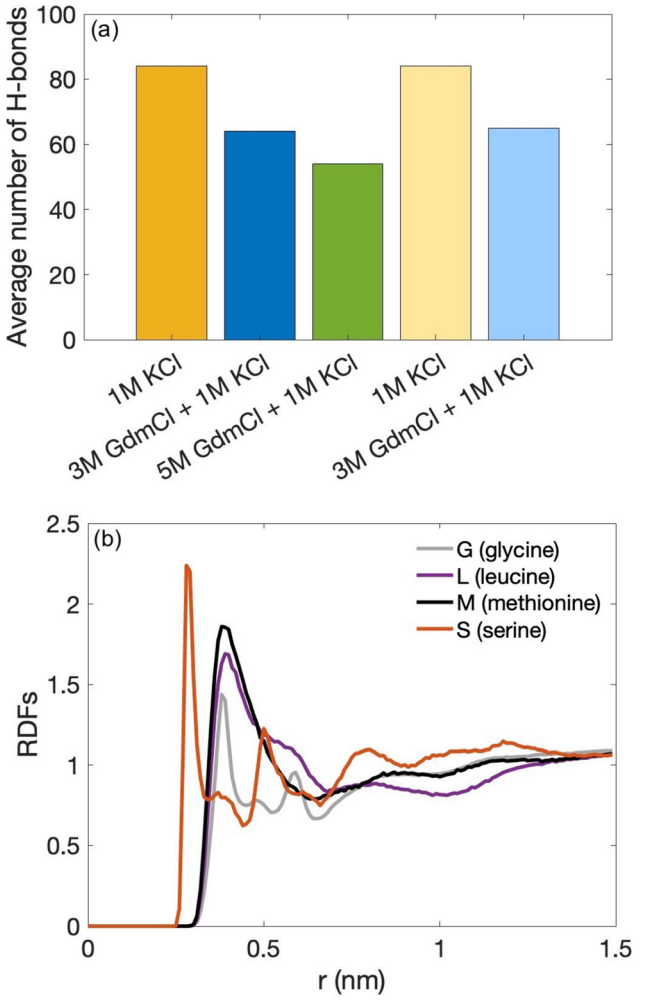

Fig. 4 (a) The average number of hydrogen bonds between the protein and water in the graphene (dark colors) and MoS_2 (light colors) nanopores. The solution type is marked in the *x*-axis. (b) The RDFs between Gdm^+ ions and atoms at the end of different amino acids denoted in the legend in a 1 M KCl solution with 3 M GdmCl.

These results apparently reveal the enhanced interplay of the biomolecule and the ions in more complex electrolyte solutions that can be utilized to stretch and linearize the protein. The trends in this interplay as we move from an elemental to a molecular electrolyte solution can be compared through the RDFs between the ions and different amino acids of the protein. In the case of the graphene pore, these are visualized in Fig. 4(b), which specifically shows the interaction of the N atoms of Gdm^+ ions and the atoms at the end of the amino acids. For the latter, we representatively take glycine, leucine, methionine, and serine. (Additional RDFs can be found in the ESI.†) The RDF peaks at different positions denote an accumulation of the Gdm^+ ions at different distances around the amino acids. These differences are more significant when comparing S with G, L, and M. In fact for the latter three, the first RDF peaks are almost at the same distance from the end of the amino acids. All amino acids accumulate within 5 Å around the protein, reducing in this way the inter-protein interactions and thus enabling linearization. The stronger interaction of the molecular cations and serine evident from the larger peak at a shorter distance is correlated with the stronger polarity of this amino acid compared to the other three on the graph, which are all non-polar. These results imply that the addition of a molecular solute should lead to a more effective linearization of the protein when this is made of many polar amino acids.

The observed strong interaction of the Gdm^+ ions and the protein should intuitively also influence the dynamics of the protein and through this all other species in the solution. In order to assess this, we provide in Fig. 5 the dynamics of the mean squared displacements of the protein (panel (a)) and the ions (panel (b)). First inspection of the MSD curves reveals a clear difference of the translocation dynamics of the protein in each medium and nanopore material. A linear MSD indicates a smooth and unidirectional translocation behavior, while quasi-linear and non-linear patterns suggest strong interactions with the nanopore surface or conformational changes in the protein structure. In the 3 M GdmCl + 1 M KCl system and the graphene nanopore, the linear MSD reflects a smooth translocation with a relatively uniform speed. In contrast, the non-linear MSD observed for 1 M KCl and the graphene nanopore suggests a bi-directional and irregular movement of the protein segment. Quasi-linear behavior, such as that seen in the 1 M KCl case for the MoS_2 nanopore, suggests that while translocation is steady over short periods, it is interrupted by unstable or fluctuating movements. These dynamics were also

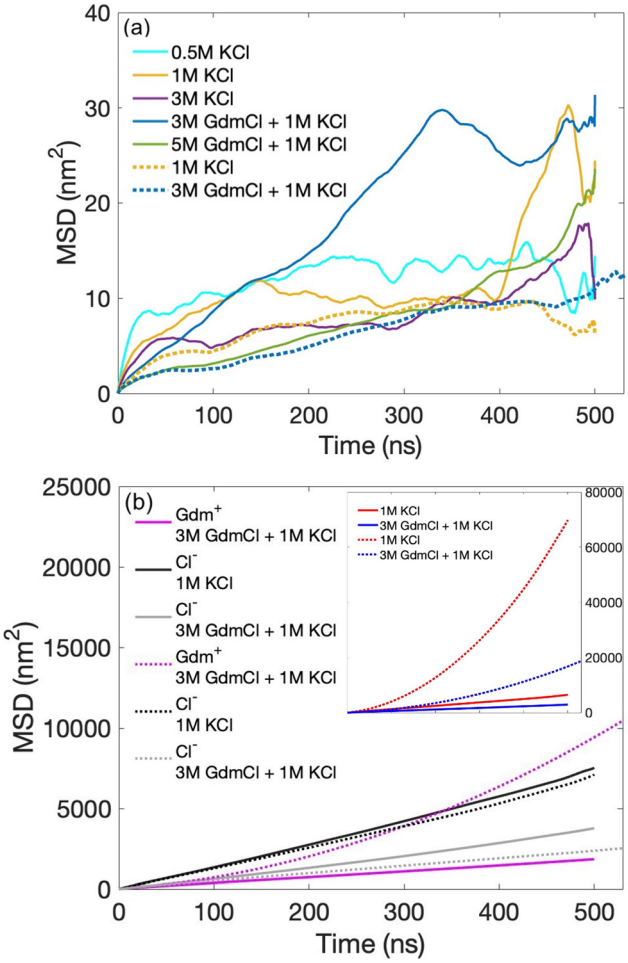

Fig. 5 Mean squared displacements of the (a) protein and (b) Gdm^+ ions, Cl^- ions, and (in the inset) K^+ ions for the graphene (solid lines) and MoS_2 (dotted lines) nanopores, respectively, and the solvent and species described in the legends. The *x*-axes of the inset and the main graph in (b) have the same scale.

observed through the visualization of the translocation trajectories.

Overall, the MSD profiles for the 3 M (solid blue) and 5 M (solid green) GdmCl in 1 M KCl increase uniformly with time for the graphene nanopore case, meaning that adding GdmCl to the electrolyte solution accelerates the protein translocation and improves the translocation dynamics. In contrast to this, the MSD profiles for the KCl solution (solid cyan, orange, and purple lines) reveal a 2- to 3-fold slower dynamics, indicating that the translocation is hindered, which could be assigned to the stickiness of graphene discussed above. Combining this information with the visualization of the respective translocation trajectories (snapshots of which are shown in Fig. 3), sticking of the protein on the graphene surface is indeed observed in pure KCl solution. Furthermore, the protein formed a hairpin structure in the 3 M KCl solution and hindered the translocation in the time frame of 60–350 ns. This matches with the fact that the respective MSD profile has almost reached a plateau within this time window. In the case of the MoS_2 nanopore, the protein dynamics are much slower, revealing a 3-fold slowing down in the 3 M GdmCl + 1 M KCl solution compared to the graphene nanopore. This can be traced back to the different charged states of the pore surface, with that of MoS_2 being negatively charged. In contrast to the graphene nanopore, no significant changes in the protein dynamics could be observed between the 1 M KCl and 3 M GdmCl + 1 M KCl solutions.

At the same time, the MSD profiles, and thus also the dynamics in the 1 M KCl solution, are of the same order for both nanopore materials. To further unravel the dynamics of the ions involved in the translocation process, we provide in Fig. 5(b) their MSD profiles. Evidently, the diffusion rates of all ions decrease with increasing ion concentration in the solution. The lighter potassium cations (see the inset) are the most mobile ones, especially when these are placed in the environment of the negatively charged MoS_2 pore. Intuitively, the chlorine anions are also more mobile than the bulkier molecular guanidinium cations, but not in the case of the MoS_2 pore as this interacts strongly with the guanidinium cations. In the 1 M KCl solution, the chlorine anions are similarly mobile for both nanopores, but show small differences in the 3 M GdmCl + 1 M KCl solution, revealing a roughly 30% higher mobility in the latter and the graphene nanopore. The reason underlying this trend is again the negatively charged MoS_2 material together with the larger Cl^- concentration and the respective increase in the electrostatic repulsive forces that occurs. Note that in Fig. 5, we also provide the results from additional KCl concentrations of 0.5 M and 3 M KCl in order to both further assess the influence of pure KCl electrolytes on the translocation dynamics and maintain a similar number of ions in the solution compared to those with GdmCl added to the 1 M KCl electrolyte. This allows us to rule out the possibility that the observed protein linearization and reduced protein adhesion are simply imposed simply by the increased number of ions in the solution.

3.3 Read-out signals: quality and solvent

The results presented above attempt to provide a detailed insight into the interplay of the pore material, protein analyte, and electrolyte solution. The main objective, though, is to connect these to the read-out characteristics of the protein by the nanopore and provide information towards enhancing this read-out in real sequencing applications. The observable that can connect all these is the ionic current traces through a nanopore, which are used experimentally to detect, identify, and sequence biomolecules.[49–51] Here, we have used the MD trajectories of the translocation process of the protein in different solutions and the two nanopore materials to calculate the ionic currents and summarize the results in Fig. 6. First, the total translocation time, known as the dwell time, of the target protein refers to the duration of a blockade current, *i.e.* the duration from the open up to the blocked current and back to the open. We have started our simulations simultaneously to the translocation, thus measuring the dwell time

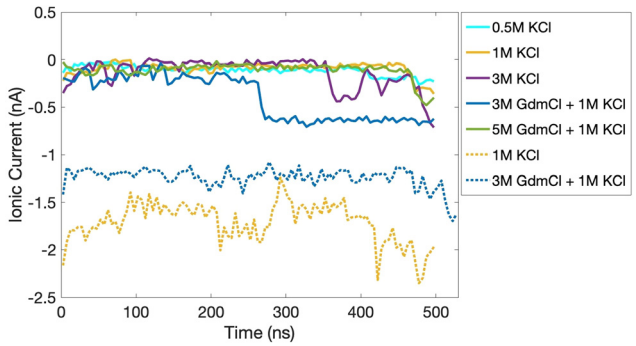

Fig. 6 Ionic current traces of a translocating protein in different solutions for both the graphene (solid lines) and MoS_2 (dotted lines) nanopores. The current was sampled at 10 ps intervals and averaged every 5 ns.

until we observe a strong transition in the ionic current traces. Note that 0 nA refers to the open current, *i.e.* the baseline in the experiments. According to this and the ionic current traces in the figure, the translocation times of the peptide through the graphene nanopore in 0.5 M, 1 M, and 3 M KCl solutions are 470 ns, 468 ns and 483 ns, respectively, while in the 3 M and 5 M GdmCl with 1 M KCl, these dwell times reduce to 266 ns and 470 ns, respectively. Obviously, adding 3 M GdmCl to the 1 M KCl solution provides a 2-fold speed-up of the translocation process in the case of the graphene pore. Notably, the non-uniform ionic current profile in the 3 M KCl solution beyond 330 ns is assigned to the formation of the hairpin protein conformation mentioned above. The difference in the ionic currents for the 3 M GdmCl + 1 M KCl concentration and the graphene nanopore is due to its unique translocation dynamics compared to the other electrolyte solutions. The blockade current is higher in this case due to the enhanced translocation dynamics of the protein segment facilitated by the presence of 3 M GdmCl. This improvement in translocation reduces the duration of obstruction within the nanopore, leading to a sharp decrease in current at around 266 ns. This decrease denotes the end of the translocation, after which the current stabilizes to the open current level.

In the case of the MoS_2 nanopore, the ionic current is comparably larger than those calculated in the graphene case due to its much higher K^+ mobility (refer to Fig. 5(b)). Interestingly, for the MoS_2 material and the 1 M KCl solution, the fluctuating ionic current traces (dotted yellow line) indicate a step-wise translocation of the protein, which can be utilized for ensuring a controlled read-out. It is also noted that the ionic currents from the MoS_2 nanopore are fluctuating more than in the graphene pore, which provides more regular currents at the end of the translocation that can be better detected and would be more effectively analyzed with regard to read-out. Overall, the ionic current in MoS_2 nanopores is much higher than in graphene nanopores, which could be attributed to the increased ion mobility due to interactions with the charged MoS_2 surface. The combined interaction of the electric field, ions, and the charged MoS_2 surface significantly contributes to this current-amplifying effect compared to the graphene case.

As mentioned in the previous sections, the Gdm^+ ions tend to form a hydrophilic layer on the graphene surface due to dispersion interactions and thus prevent the sticking of the protein to the graphene during translocation. At the same time, the higher the guanidinium concentration, the lower the overall dynamics (refer to the MSD in Fig. 5). We next aim to obtain the minimum effective concentration of GdmCl that can linearize the protein and, at the same time, sustain the translocation process and the corresponding ionic currents. For this, we have compared the results for the 1 M KCl solution by adding 1 M, 2 M and 3 M GdmCl, respectively, in the case of the graphene pore. By comparing the radius of gyration (the respective time evolution can be found in the ESI†) and the current traces from these simulations, we concluded that a GdmCl concentration below 3 M is not efficient for either hindering the stickiness of graphene or sufficiently linearizing the protein. On the other end, when increasing the GdmCl concentration to 5 M, the dwell time is comparable to that in a pure 1 M KCl solution. Accordingly, larger GdmCl concentrations do slow down the translocation. We thus conclude that the addition of 3 M and up to 5 M GdmCl is the optimal condition of those studied here for the case of the graphene nanopore. Interestingly, for the 3 M GdmCl + 1 M KCl solution, once we deduct the number of Gdm^+ ions that form the hydrophilic layer on graphene (thus preventing any peptide adhesion) from the total guanidinium number in the solution, the remaining concentration of GdmCl is roughly 2.5 M, which is comparable to the previously reported minimum effective GdmCl concentration of 2 M to unfold a protein translocating a α-hemolysin biological nanopore.[27]

4 Conclusions

Using a histone protein segment, we have investigated its translocation characteristics in two different pores and electrolyte environments. We were able to tackle and resolve two challenges: the protein adhesion on graphene and its 3D conformation in a liquid environment. The adhesion of the amino acids on the graphene pore surface was avoided by adding a molecular solute, such as GdmCl, to a typical simple electrolyte solution. The optimal concentration of GdmCl was found in the range 3–5 M. In these solutions, the guanidinium cations form a hydrophilic ionic layer on the graphene surface, inhibiting protein adhesion. At the same time, the molecular cations intervene in the strong intra-protein interactions, effectively promoting the linearization of the protein. The linearization, in turn, promotes a single-file translocation considerably influencing the read-out possibilities, as the amino acids can be detected one by one. Graphene nanopores cannot operate well under normal conditions of simple electrolyte solutions, but in the presence of the denaturant, they promote faster protein dynamics, while also providing a more regular ionic current with a clear start and end of the translocation as in the

case of MoS_2 nanopores. The latter, though, can translocate the analytes even under normal conditions, providing slower protein translocation and a roughly 2-fold enhancement of the detectable ionic current, but a lower degree of protein linearization. Charged nanopores considerably enhance the mobility of counter ions, which can be translated to stronger ionic currents. At the same time, bulkier molecular ions might interact strongly with the amino acids, but can clog the nanopores at high concentrations, reducing the dynamics of all species in the process. In the end, the aim of this work was to investigate conditions that improve the nanopore setting and optimize the translocation process. The next step would be to move towards resolving ionic currents at the single nucleotide or amino acid level, typically performed using machine learning tools. Our detailed analysis of the interplay of the material type and solution characteristics and their distinct influence on protein linearization and nanopore currents is key in optimizing the nanopore setup in view of detecting proteins and post-translational modifications therein.

Data availability

The data generated and analyzed in this work can be made available upon any reasonable request.

Conflicts of interest

There are no conflicts to declare.

Acknowledgements

The authors are thankful to Amir Barati Farimani and Chandan K. Das for useful discussions. The computing time provided at the NHR Center NHR4CES at RWTH Aachen University (project number p0020207) is greatly acknowledged. This work was funded by the Federal Ministry of Education and Research and the state governments participating on the basis of the resolutions of the GWK for national high performance computing at universities. This work is part of the nanodiagBW consortium (project numbers 03ZU1208BI and 03ZU1208AJ) funded by the German Federal Ministry of Education and Research (BMBF) within the Clusters4Future initiative. Funding from the German Funding Agency (Deutsche Forschungsgemeinschaft-DFG) under the project "novel complex nanopores for the detection of natural and mutated DNA" (project number 508324943) is greatly acknowledged.

References

1 M. Rhee and M. A. Burns, Nanopore sequencing technology: Nanopore preparations, *Trends Biotechnol.*, 2007, **25**(4), 174–181.
2 J.-H. Ahn, B. H. Hong, F. Torrisi, J. N. Coleman, J. Liu, S. Böhm, M. Drndić, K. Kostarelos, K. S. Novoselov and E. J. Siochi, Things you could do with graphene, *Nat. Nanotechnol.*, 2014, **9**, 737–747.
3 H. Chen, L. Li, T. Zhang, Z. Qiao, J. Tang and J. Zhou, Protein translocation through a MoS_2 nanopore: A molecular dynamics study, *J. Phys. Chem. C*, 2018, **122**(4), 2070–2080.
4 G. F. Schneider, S. W. Kowalczyk, V. E. Calado, G. Pandraud, H. W. Zandbergen, L. M. Vandersypen and C. Dekker, DNA translocation through graphene nanopores, *Nano Lett.*, 2010, **10**(8), 3163–3167.
5 C. A. Merchant, K. Healy, M. Wanunu, V. Ray, N. Peterman, J. Bartel, M. D. Fischbein, K. Venta, Z. Luo, A. T. Charlie Johnson, *et al.*, DNA translocation through graphene nanopores, *Nano Lett.*, 2010, **10**(8), 2915–2921.
6 S. Garaj, W. Hubbard, A. Reina, J. Kong, D. Branton and J. A. Golovchenko, Graphene as a subnanometre trans-electrode membrane, *Nature*, 2010, **467**(7312), 190–193.
7 T. Zhang, *Discovery of Graphene*, Springer Singapore, Singapore, 2022, pp. 1–15.
8 K. Liu, J. Feng, A. Kis and A. Radenovic, Atomically thin molybdenum disulfide nanopores with high sensitivity for DNA translocation, *ACS Nano*, 2014, **8**(3), 2504–2511.
9 M. Graf, M. Lihter, M. Thakur, V. Georgiou, J. Topolancik, B. R. Ilic, K. Liu, J. Feng, Y. Astier and A. Radenovic, Fabrication and practical applications of molybdenum disulfide nanopores, *Nat. Protoc.*, 2019, **14**(4), 1130–1168.
10 M. Graf, M. Lihter, D. Altus, S. Marion and A. Radenovic, Transverse detection of dna using a MoS_2 nanopore, *Nano Lett.*, 2019, **19**(12), 9075–9083.
11 F. Wang, C. Zhao, P. Zhao, F. Chen, D. Qiao and J. Feng, MoS_2 nanopore identifies single amino acids with sub-1 dalton resolution, *Nat. Commun.*, 2023, **14**(1), 2895.
12 A. Barati Farimani, M. Heiranian and N. R. Aluru, Identification of amino acids with sensitive nanoporous MoS_2: Towards machine learning-based prediction, *npj 2D Mater. Appl.*, 2018, **2**(1), 14.
13 D. B. Wells, M. Belkin, J. Comer and A. Aksimentiev, Assessing graphene nanopores for sequencing DNA, *Nano Lett.*, 2012, **12**(8), 4117–4123.
14 R. L. Kumawat and B. Pathak, Individual identification of DNA nucleobases on atomically thin black phosphorene nanoribbons: van der Waals corrected density functional theory calculations, *J. Phys. Chem. C*, 2019, **123**(36), 22377–22383.
15 J. Wilson, L. Sloman, Z. He and A. Aksimentiev, Graphene nanopores for protein sequencing, *Biophys. J.*, 2016, **110**(3), 326a.
16 S. Mittal, R. L. Kumawat, M. K. Jena and B. Pathak, Graphene nanoslit device for protein sequencing: Ab initio quantum transport study, *ACS Appl. Nano Mater.*, 2022, **5**(2), 2715–2727.
17 R. L. Kumawat, M. K. Jena and B. Pathak, Individual identification of amino acids on an atomically thin hydrogen

boride system using electronic transport calculations, *J. Phys. Chem. C*, 2020, **124**(49), 27194–27202.
18 D. B. Wells, M. Belkin, J. Comer and A. Aksimentiev, Assessing graphene nanopores for sequencing DNA, *Nano Lett.*, 2012, **12**(8), 4117–4123.
19 Y. P. Shan, P. B. Tiwari, P. Krishnakumar, I. Vlassiouk, W. Z. Li, X. W. Wang, Y. Darici, S. M. Lindsay, H. D. Wang, S. Smirnov, *et al.*, Surface modification of graphene nanopores for protein translocation, *Nanotechnology*, 2013, **24**(49), 495102.
20 Z. Tang, B. Lu, Q. Zhao, J. Wang, K. Luo and D. Yu, Surface modification of solid-state nanopores for sticky-free translocation of single-stranded DNA, *Small*, 2014, **10**(21), 4332–4339.
21 W. Si, Y. Zhang, G. Wu, Y. Kan, Y. Zhang, J. Sha and Y. Chen, Discrimination of protein amino acid or its protonated state at single-residue resolution by graphene nanopores, *Small*, 2019, **15**(14), 1900036.
22 B. Luan and R. Zhou, Single-file protein translocations through graphene–MoS_2 heterostructure nanopores, *J. Phys. Chem. Lett.*, 2018, **9**(12), 3409–3415.
23 Q. Zhong, X. Xiao, Y. Qiu, Z. Xu, C. Chen, B. Chong, X. Zhao, S. Hai, S. Li, Z. An, *et al.*, Protein posttranslational modifications in health and diseases: Functions, regulatory mechanisms, and therapeutic implications, *MedComm*, 2023, **4**(3), e261.
24 H. Brinkerhoff, A. S. Kang, J. Liu, A. Aksimentiev and C. Dekker, Multiple rereads of single proteins at single-amino acid resolution using nanopores, *Science*, 2021, **374**(6574), 1509–1513.
25 P. Masson and S. Lushchekina, Conformational stability and denaturation processes of proteins investigated by electrophoresis under extreme conditions, *Molecules*, 2022, **27**(20), 6861.
26 O. I. Povarova, I. M. Kuznetsova and K. K. Turoverov, Differences in the pathways of proteins unfolding induced by urea and guanidine hydrochloride: molten globule state and aggregates, *PLoS One*, 2010, **5**(11), e15035.
27 L. Yu, X. Kang, F. Li, B. Mehrafrooz, A. Makhamreh, A. Fallahi, J. C. Foster, A. Aksimentiev, M. Chen and M. Wanunu, Unidirectional single-file transport of full-length proteins through a nanopore, *Nat. Biotechnol.*, 2023, **41**(8), 1130–1139.
28 K. Motone, N. Cardozo and J. Nivala, Herding cats: Label-based approaches in protein translocation through nanopore sensors for single-molecule protein sequence analysis, *iScience*, 2021, **24**, 103032.
29 Z.-L. Hu, M.-Z. Huo, Y.-L. Ying and Y.-T. Long, Biological nanopore approach for single-molecule protein sequencing, *Angew. Chem., Int. Ed.*, 2021, **60**, 14738–14749.
30 M. J. Abraham, T. Murtola, R. Schulz, S. Páll, J. C. Smith, B. Hess and E. Lindahl, Gromacs: High performance molecular simulations through multi-level parallelism from laptops to supercomputers, *SoftwareX*, 2015, **1**, 19–25.
31 K. Vanommeslaeghe, E. Hatcher, C. Acharya, S. Kundu, S. Zhong, J. Shim, E. Darian, O. Guvench, P. Lopes, I. Vorobyov, *et al.*, Charmm general force field: A force field for drug-like molecules compatible with the charmm all-atom additive biological force fields, *J. Comput. Chem.*, 2010, **31**(4), 671–690.
32 W. L. Jorgensen, J. Chandrasekhar, J. D. Madura, R. W. Impey and M. L. Klein, Comparison of simple potential functions for simulating liquid water, *J. Chem. Phys.*, 1983, **79**(2), 926–935.
33 T. R. Walsh, *et al.*, Predicting biomolecule adsorption on MoS_2 nanosheets with high structural fidelity, *Chem. Sci.*, 2022, **13**(18), 5186–5195.
34 J. Liu, J. Zeng, C. Zhu, J. Miao, Y. Huang and H. Heinz, Interpretable molecular models for molybdenum disulfide and insight into selective peptide recognition, *Chem. Sci.*, 2020, **11**(33), 8708–8722.
35 Z. Gu, Z. Yang, S.-G. Kang, J. R. Yang, J. Luo and R. Zhou, Robust denaturation of villin headpiece by MoS_2 nanosheet: Potential molecular origin of the nanotoxicity, *Sci. Rep.*, 2016, **6**(1), 28252.
36 G. Bussi, D. Donadio and M. Parrinello, Canonical sampling through velocity rescaling, *J. Chem. Phys.*, 2007, **126**(1), 014101.
37 M. Parrinello and A. Rahman, Polymorphic transitions in single crystals: A new molecular dynamics method, *J. Appl. Phys.*, 1981, **52**(12), 7182–7190.
38 B. Hess, H. Bekker, H. J. Berendsen and J. G. Fraaije, Lincs: A linear constraint solver for molecular simulations, *J. Comput. Chem.*, 1997, **18**(12), 1463–1472.
39 T. Darden, D. York and L. Pedersen, Particle mesh Ewald: An n log (n) method for ewald sums in large systems, *J. Chem. Phys.*, 1993, **98**(12), 10089–10092.
40 W. Humphrey, A. Dalke and K. Schulten, VMD – Visual molecular dynamics, *J. Mol. Graphics*, 1996, **14**, 33–38.
41 J. J. Kasianowicz, E. Brandin, D. Branton and D. W. Deamer, Characterization of individual polynucleotide molecules using a membrane channel, *Proc. Natl. Acad. Sci. U. S. A.*, 1996, **93**(24), 13770–13773.
42 D. W. Deamer and M. Akeson, Nanopores and nucleic acids: Prospects for ultrarapid sequencing, *Trends Biotechnol.*, 2000, **18**(4), 147–151.
43 M. Farshad and J. C. Rasaiah, Molecular dynamics simulation study of transverse and longitudinal ionic currents in solid-state nanopore DNA sequencing, *ACS Appl. Nano Mater.*, 2020, **3**(2), 1438–1447.
44 L. Wu, H. Liu, W. Zhao, L. Wang, C. Hou, Q. Liu and Z. Lu, Electrically facilitated translocation of protein through solid nanopore, *Nanoscale Res. Lett.*, 2014, **9**, 1–10.
45 O. M. Eggenberger, C. Ying and M. Mayer, Surface coatings for solid-state nanopores, *Nanoscale*, 2019, **11**(42), 19636–19657.
46 X. Zeng, Y. Xiang, Q. Liu, L. Wang, Q. Ma, W. Ma, D. Zeng, Y. Yin and D. Wang, Nanopore technology for the application of protein detection, *Nanomaterials*, 2021, **11**(8), 1942.
47 M. Y. Lobanov, N. S. Bogatyreva and O. V. Galzitskaya, Radius of gyration as an indicator of protein structure compactness, *Mol. Biol.*, 2008, **42**, 623–628.
48 S. B. Syed, F. I. Khan, S. H. Khan, S. Srivastava, G. M. Hasan, K. A. Lobb, A. Islam, M. I. Hassan and

F. Ahmad, Unravelling the unfolding mechanism of human integrin linked kinase by gdmcl-induced denaturation, *Int. J. Biol. Macromol.*, 2018, **117**, 1252–1263.

49 A. Meller, L. Nivon and D. Branton, Voltage-driven DNA translocations through a nanopore, *Phys. Rev. Lett.*, 2001, **86**(15), 3435.

50 J. Li, M. Gershow, D. Stein, E. Brandin and J. A. Golovchenko, DNA molecules and configurations in a solid-state nanopore microscope, *Nat. Mater.*, 2003, **2**(9), 611.

51 C. Dekker, Solid-state nanopores, *Nat. Nanotechnol.*, 2007, **2**(4), 209–215.